

## Comparative assessment of seismic rehabilitation techniques on a full scale 3-story RC moment frame structure

M. Di Ludovico<sup>†</sup>, A. Balsamo<sup>‡</sup>, A. Prota<sup>††</sup> and G. Manfredi<sup>‡‡</sup>

*Department of Structural Engineering, University of Naples Federico II, 80125, Naples, Italy*

*(Received October 25, 2006, Accepted February 18, 2008)*

**Abstract.** In the framework of the SPEAR (Seismic PERFORMANCE Assessment and Rehabilitation) research Project, an under-designed three storey RC frame structure, designed to sustain only gravity loads, was subjected, in three different configurations 'as-built', Fiber Reinforced Polymer (FRP) retrofitted and rehabilitated by reinforced concrete (RC) jacketing, to a series of bi-directional pseudo-dynamic (PsD) tests under different values of peak ground acceleration (PGA) (from a minimum of 0.20g to a maximum of 0.30g). The seismic deficiencies exhibited by the 'as-built' structure after the test at PGA level of 0.20g were confirmed by a post – test assessment of the structural seismic capacity performed by a nonlinear static pushover analysis implemented on the structure lumped plasticity model. To improve the seismic performance of the 'as-built' structure', two rehabilitation interventions by using either FRP laminates or RC jacketing were designed. Assumptions for the analytical modeling, design criteria and calculation procedures along with local and global intervention measures and their installation details are herein presented and discussed. Nonlinear static pushover analyses for the assessment of the theoretical seismic capacity of the structure in each retrofitted configuration were performed and compared with the experimental outcomes.

**Keywords:** full-scale; RC; seismic retrofit; GFRP; concrete jacketing; biaxial bending; nonlinear push-over analysis.

---

### 1. Introduction

The most strictly connected aspect to the hazard in southern European countries is represented by a number of existing RC structures under-designed or designed following old codes and construction practice. Casualties and losses are mainly due to deficient RC buildings not adequately designed for earthquake resistance. Since such buildings represent the majority of the existing structures, the assessment of structurally effective rehabilitation schemes is nowadays strictly necessary. In this context, the SPEAR (Seismic PERFORMANCE Assessment and Rehabilitation) research Project, specifically targeted at evaluation of current assessment and rehabilitation methods

---

<sup>†</sup> Assistant Professor, Ph.D., Corresponding author, E-mail: [diludovi@unina.it](mailto:diludovi@unina.it)

<sup>‡</sup> E-mail: [albalsam@unina.it](mailto:albalsam@unina.it)

<sup>††</sup> E-mail: [aprota@unina.it](mailto:aprota@unina.it)

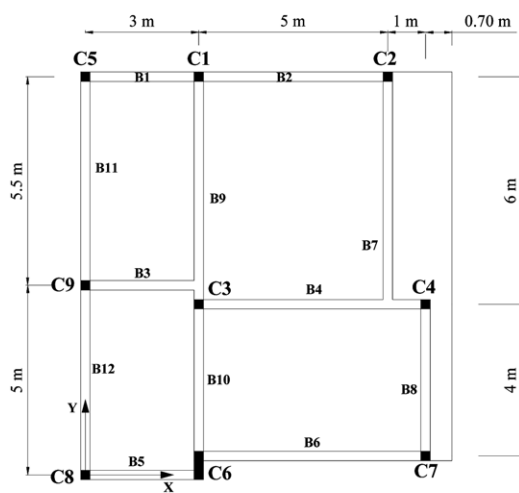
<sup>‡‡</sup> E-mail: [gamanfre@unina.it](mailto:gamanfre@unina.it)

and at development of new assessment and retrofitting techniques, was developed at the Join Research Center (JRC) in Ispra (Italy). The research project consisted of a series of full-scale bi-directional pseudo-dynamic (PsD) tests on an under-designed three storey RC framed structure; PsD tests consist of simultaneous application of the longitudinal and the transverse earthquake components to the structure (a detailed description of both the method and the mathematical approach can be found in Molina *et al.* 1999, Molina *et al.* 2004).

The structure, that represents a simplification of a typical old construction in Southern Europe, was designed to sustain only gravity loads with deficiencies typical of non-seismic existing buildings as plan irregularity, poor local detailing, scarcity of rebars, insufficient column confinement, weak joints and older construction practice; design strengths of concrete and smooth steel bars were equal to  $f_c' = 25$  MPa and  $f_y = 320$  MPa, respectively.

The structure is regular in elevation with a storey height of 3 meters and 2.5 m clear height of columns between the beams; it is non symmetric in both directions, with 2-bay frames spanning from 3 to 6 meters. The plan layout and the 3D view of the structure are shown in Fig. 1. The concrete floor slabs are 150 mm thick, with bi-directional 8 mm smooth steel rebars, at 100, 200 or 400 mm spacing. Beam cross-sections are 250 mm wide and 500 mm deep. Eight of the nine columns have a square 250 by 250 mm cross-section; the ninth (column C6) has a rectangular cross-section of 250 by 750 mm, which makes it much stiffer and stronger than the others along the Y direction which is the strong direction for the whole structure. The joints of the structure are one of its weakest points: neither beam nor column stirrups continue into them, so that no confinement at all is provided. Moreover, some of the beams directly intersect other beams (see joint close to columns C3 and C4 in Fig. 1) resulting in beam-to-beam joints without the support of the column. Details about beams and columns reinforcement for flexure and shear can be found in Negro *et al.* (2004).

The 'as-built' structure was initially subjected to a bi-directional PsD test in the ELSA laboratory of the JRC under the Montenegro Hercegovina record scaled to a PGA of 0.20g. After that a post-



(a)



(b)

Fig. 1 Plan view (a) and 3D view (b) of the SPEAR structure

test lumped plasticity model of the structure was implemented in order to assess the theoretical seismic capacity of the structure. Since both theoretical and experimental results showed that the 'as-built' structure was unable to withstand a larger seismic action, it was decided to investigate on the effectiveness of two of the main available rehabilitation strategies (Thermou and Elnashai, 2006): 1) by using FRP laminates and 2) by RC jacketing.

Both rehabilitation intervention, by increasing only the global structural ductility in the former case and both ductility and strength in the latter case, were designed with reference to the earthquake demand correlated to a PGA level of 0.30g. The background, the philosophy and the calculations procedures followed to carry out the design of the GFRP retrofit and the RC jacketing are herein presented and discussed. The design of the adopted local and global intervention measures has been supported by nonlinear static pushover analyses implemented by a lumped plasticity model of the structure in each retrofitted configuration. The finite element analysis program SAP 2000, very commonly used by structural engineering practitioners, was used to run the theoretical analyses.

The rehabilitation design compliance with the acceptance criteria for the selected objective and its effectiveness are herein explored and discussed by the comparison with the experimental results provided by a new series of tests (two for each configuration) performed on the full-scale rehabilitated structure with the same input accelerogram selected for the 'as built' specimen but scaled to a PGA value of 0.20g and 0.30g, respectively.

## 2. Behavior of the 'as-built' structure

### 2.1 Test at 0.20g PGA level

The experimental activity started by testing the 'as-built' structure with a scaled PGA level of 0.20g. The results of such test showed that the major damage concerned the ends of the square columns with crushing of concrete at all stories. The level of damage was more significant at the second storey. For each floor, the most damaged members were the columns. During tests, significant cracks opened on the tensile side of the columns at the beam-column interface. The damage on the rectangular column C6 was less significant even though crushing of concrete and cracks at the interface with beams were observed. Details about the experimental performance of the 'as-built' structure can be found in Negro *et al.* (2004). The experimental outcomes in terms of maximum base shear and top displacement along with the maximum inter-storey drifts for the longitudinal direction (positive and negative X-direction, named PX and NX, respectively) and in the transverse direction (positive and negative Y-direction, named PY and NY, respectively) are summarized in Table 1 (positive and negative direction are referred to the coordinate system of Fig. 1).

The table shows that the maximum base shear was reached along the Y direction, 276 kN, rather than in the X one, 195 kN; such result was consistent with the arrangement of the wall type column C6 placed with its strong axis in such direction. On the contrary, much larger top displacements were reached in the X direction, 0.1057 m, rather than in the Y direction where a maximum top displacement equal to 0.1031 m was achieved. According to the observed damages the maximum inter-storey drifts were reached at the second storey (0.0570 m in the X and 0.0472 m in the Y direction, respectively).

Table 1 Experimental outcomes in the 'as-built' configuration

	Test	Max Base Shear [KN]	Max Top Displ. [m]	Level	Max I-S Displ. [m]
X Dir.	as-built' 0.2g	PX: 184	PX: 0.1057	1	0.0246
		NX: 195	NX: 0.0919	2	0.0570
				3	0.0358
Y Dir.	as-built' 0.20g	PY: 261	PX: 0.1031	1	0.0306
				2	0.0472
		NY: 276	NX: 0.0920	3	0.0326

## 2.2 Post-test assessment: Lumped plasticity model of the structure

A post-test assessment of the structural global capacity was performed by a non-linear static pushover analysis on the 'as-built' structure. Pushover analyses in the longitudinal and transverse directions were performed by subjecting the structure to a monotonically increasing pattern of lateral forces related to modes of vibration and mass distribution; in particular, as the participating masses were  $M_{\%X} = 72\%$  and  $M_{\%Y} = 6\%$  in the 1<sup>st</sup> mode of vibration and  $M_{\%X} = 12\%$  and  $M_{\%Y} = 61\%$  in the 2<sup>nd</sup> mode, lateral forces proportional to the 1<sup>st</sup> and 2<sup>nd</sup> mode of vibration were assumed in the X and Y directions, respectively. Lateral loads were applied at the location of the centre of masses in the model. In the analytical model slabs were omitted and their contribution to beam stiffness and strength was considered assuming a T cross section for the beams with the effective flange width equal to the rectangular beam width (250 mm) plus 7% of the clear span of the beam on either side of the web (Fardis1994, Jeong and Elnashai 2005).

The inelastic flexural behaviour of elements was considered by modelling the structural members with lumped plasticity at both ends; a bilinear moment-rotation relationship was used for each plastic hinge. The moment rotation relationship was obtained based on the moment curvature analysis performed for each element cross-section considering section properties and constant axial loads (due to gravity loads) for columns and axial forces equal to zero for the beams. It is noted that the ultimate curvature,  $\phi_u$ , and ultimate moment,  $M_u$ , were determined in correspondence of the attainment of ultimate strains in concrete or steel (concrete ultimate strain was conventionally assumed equal to 3.5‰; the steel ultimate strain was conventionally assumed equal to 40‰).

Plastic hinge length,  $L_{pl}$ , yielding and ultimate rotation,  $\theta_y$  and  $\theta_u$ , were computed according to the Eurocode 8 *Part 3*, 2003 type expressions; in particular the equations provided by the latest seismic guideline developed by the Italian Department of Civil Protection, Ordinanza 3431, 2005 were adopted. Details about modelling assumptions can be found in Di Ludovico *et al.* (2006).

## 2.3 Theoretical Capacity vs. Demand

According to the Ordinanza 3431, 2005, two limit states were investigated in order to evaluate the structural capacity: 1) the damage limit state (LSDL) which corresponds to the first attainment of  $\theta_y$  in one of the plastic hinges; 2) the significant damage limit state (LSSD) which corresponds to the first attainment of the  $0.75\theta_u$  in one of the plastic hinges. Based on such limit states, pushover analyses on the 'as-built' structure were performed in the longitudinal PX-NX direction and in the

transverse PY-NY direction (see Fig. 2); the maximum base shear and top displacement capacity for each investigated limit state are reported in Table 2.

The seismic demand was computed with reference to the Ordinanza 3431, 2005 design spectrum (soil type c, 5% damping) that provide a pseudo-acceleration spectrum compatible with that obtained by the experimental assumed ground motion record, Montenegro Herceg-Novi. Although the ‘as-built’ structure was tested under a maximum PGA level of 0.20g, the theoretical analysis of the ‘as-built’ structure was performed also for a seismic level of 0.30g in order to evaluate the theoretical structural performance in correspondence of larger seismic action intensity. Thus, in order to compute the demand, both the elastic acceleration and displacement spectrum were scaled to PGA level of 0.20g and 0.30g and plotted in acceleration-displacement (AD) format (see Fig. 3). The Capacity Spectrum Approach (CSA) was used for the seismic verification (Fajfar 2000).

The seismic demand was computed combining the pushover analysis of an equivalent multi-degree-of-freedom (MDOF) model with the response spectrum of an equivalent single-degree-of-freedom (SDOF) system. The results in terms of top displacement required for each PGA level and limit state investigated are summarized in Table 2.

Such table shows that the ‘as-built’ structure is able to satisfy both LSDL and LSSD in each direction with reference to the 0.20g PGA level even if, especially in the positive and negative X

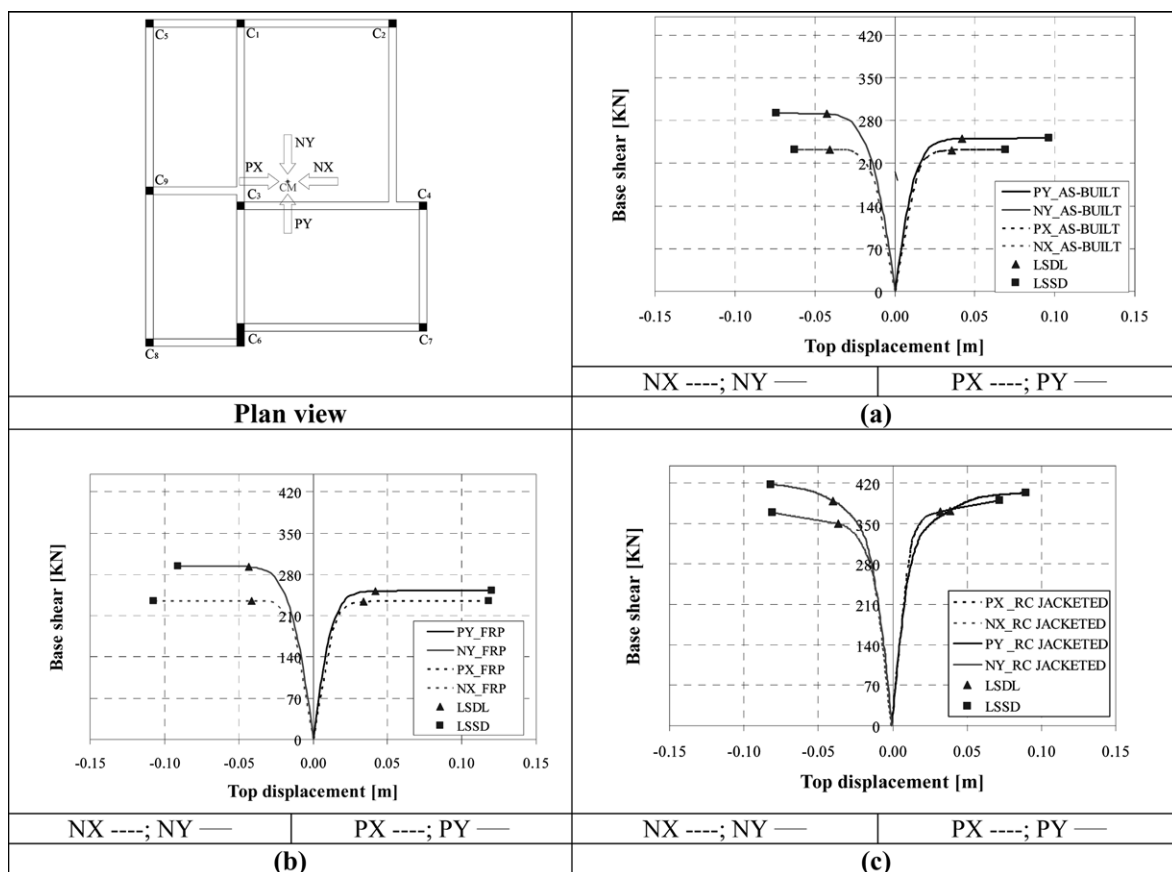


Fig. 2 Pushover curves in the ‘as-built’ (a), FRP (b) and RC jacketing (c) configurations

Table 2 Summary of the results in terms of capacity and demand for the ‘as-built’ structure

Push Direction	Limit State	‘as built’ Structure			
		Capacity		Demand	
		$F_{\max}$ [KN]	$d_{\max}$ [m]	0,20g $d_{\max}$ [m]	0,30g $d_{\max}$ [m]
PX	LSDL	231	0,0355	0,0248	0,0372 *
	LSSD	232	0,0690	0,0623	0,0934 *
NX	LSDL	232	0,0406	0,0247	0,0371
	LSSD	232	0,0626	0,0618	0,0927 *
PY	LSDL	250	0,0422	0,0240	0,0360
	LSSD	251	0,0962	0,0607	0,0910
NY	LSDL	291	0,0425	0,0240	0,0361
	LSSD	292	0,0740	0,0603	0,0904 *

(\*Demand displacements not satisfied by the structure)

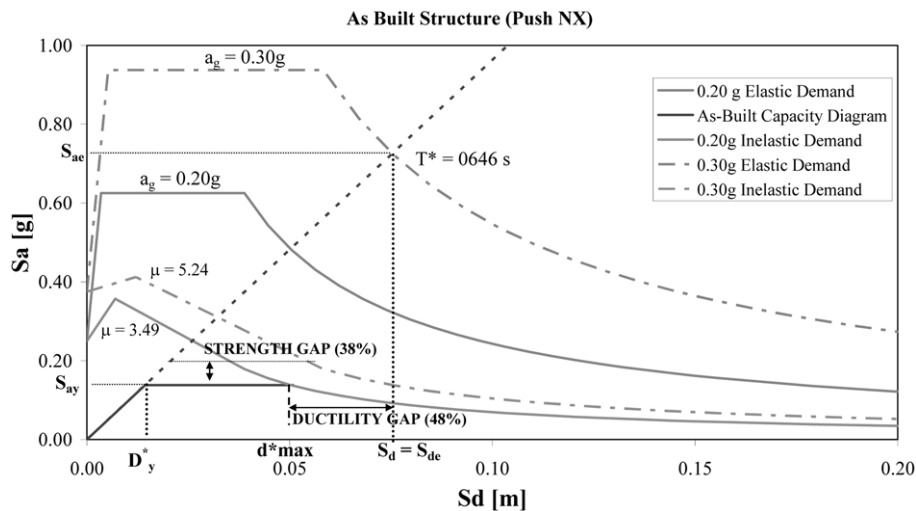


Fig. 3 ‘As-built’ structure elastic and inelastic demand spectra vs. capacity diagram

direction for the LSSD, the capacity is only slightly larger than the demand. Moreover, increasing the seismic action up to a 0.30g, the LSDL verification is not satisfied in the PX direction; with regards to the LSSD, the capacity is larger than demand only in the PY direction. At this PGA level for the LSSD the maximum gap in terms of maximum top displacement is provided in the NX direction where the difference between the seismic demand and the displacement capacity is equal to 0.0301 m (0.0927 m minus 0.0626 m) corresponding to a percentage performance gap equal to 48%. Such result is clearly highlighted by Fig. 3 in which the seismic demand, for the two levels of ground motion analysed for the equivalent SDOF system in the NX direction, is determined by using a capacity spectrum approach (Fajfar 2000).

Plotting in the same graph the demand spectra and the capacity diagram, it is possible to

determine the acceleration and the corresponding elastic displacement demand (named  $S_{ae}$  and  $S_{de}$ , respectively), required in the case of elastic behaviour, by intersecting the radial line corresponding to the elastic period of the idealized bilinear system  $T^*$  with the elastic demand spectrum. Once the ductility demand,  $\mu = S_d/D_y^*$  ( $S_d$  = requested displacement, and  $D_y^*$  = yield displacement of the idealized bilinear system of the equivalent SDOF system) is computed (depending if  $T^*$  is greater or less than  $T_C$ ), the inelastic demand in terms of accelerations and displacements is provided by the intersection point of the capacity diagram with the demand spectrum corresponding to  $\mu$ . Fig. 3 highlights that the 'as-built' structure in the NX direction, hardly able to satisfy the demand corresponding to the 0.20g PGA level, is totally lacking the appropriate capacity to resist the 0.30g PGA level as the requested ductility is about  $\mu = 5.24$  against the structural ductility equal to  $\mu_s = 3.54$  (obtained as the ratio between the maximum displacement of the of the equivalent SDOF system,  $d_{\max}^* = 0.0509$  m, and its yield displacement,  $D_y^* = 0.0143$  m).

#### 2.4 Theoretical vs. Experimental results

The theoretical analysis provided results close to the experimental ones as it predicted the first attainment of the significant damage limit state (i.e.,  $0.75\theta_u$  in the plastic hinge) in correspondence of the columns ends at the second floor (i.e., at column C3 and C4 in the PX and NX direction, respectively) where the most significant damages were found during the test. Moreover, it is noted that the theoretical analysis was in good agreement with the experimental outcomes because, according to the damage pattern found on the structure after the test, it provides a 0.20g as a limit acceleration value for the verification of the LSSD.

### 3. Design of the rehabilitation interventions

The results provided by the experimental activity and by the lumped plasticity analysis indicate that, in order to increase the seismic capacity of the structure, a rehabilitation intervention was necessary; in particular, theoretical results showed that the target design PGA level equal to 0.30g could have been sustained by 1) increasing the global deformation capacity of the structure (the displacement capacity need to be increased by a factor of 48%); 2) improving both strength and ductility capacity of the structure; 3) increasing only the strength capacity of the structure (the strength capacity needs to be increased by a factor of 38%). It is noted that such percentage values are computed according to the hypothesis that the elastic period of the idealized bilinear system,  $T^*$ , remains constant after the rehabilitation intervention.

The first two strategies outlined were chosen and pursued by using FRP laminates and RC jacketing, respectively. The design criteria used for the retrofit and the analytical predictions of the two investigated techniques are reported in the following sections.

#### 3.1 FRP Retrofit

Both experimental activity and theoretical assessment of the 'as-built' structure highlighted that columns cross-sectional dimensions and amount of longitudinal steel reinforcement were inadequate to satisfy the demand generated by the biaxial bending associated with the axial load; the weak column-strong beam condition led to the formation of plastic hinges in the columns. Since it was

decided to provide a seismic retrofit of the structure by increasing the ductility of the plastic hinges at column ends, rather than establishing a correct hierarchy of strength by their relocation, the retrofit design strategy was focused on two main aspects: 1) increasing the global deformation capacity of the structure and thus its dissipating global performance and 2) allowing to fully exploit such capacity by avoiding brittle collapses modes.

The first issue was pursued by the columns confinement that, increasing the ultimate concrete compressive strain, induces an increase of curvature ductility and thus, assuming a plastic hinge length not significantly affected by the FRP retrofit, corresponds to a proportional increase of the plastic hinge rotation capacity.

Considering that, in the case of interior application in buildings, durability performance is not the driving design criterion, it was decided, because of the reduced costs, to use glass fibers for the columns confinement. It was computed that by using two plies of uniaxial GFRP laminates with density of 900 gr/m<sup>2</sup>, thickness of dry fibers of 0.48 mm/ply, modulus of elasticity of 65.7 GPa, tensile strength of 1314 MPa applied to the square column ends, the ultimate compressive concrete strain becomes 8.87‰ (more than twice the conventional one, 3.50‰) corresponding to an increase of ultimate curvature of about 190% and rotation capacity of about 138%. Such increases were computed with reference to the central column C3 that was selected for calculations since it carries the maximum axial force due to gravity loads,  $P = 409$  kN at first story (see Di Ludovico *et al.* 2006 for details). The moment curvature relationship related to column C3 cross-section at first story in the original and GFRP confined configuration is plotted in Fig. 4; the dashed line represents the moment-curvature progress by adding one ply at a time of GFRP confinement.

Since the design goal was to allow the structure withstanding a 0.3g PGA level (theoretical analysis indicate that, for a ductility-only intervention, a 48% of structural deformation capacity increase was necessary) and recalling that the local increase of the rotation capacity is not proportional to the global deformation capacity, such amount of GFRP laminates was estimated enough for the retrofit design. Thus, based on such considerations, the first trial in the design of the GFRP confinement was chosen as 2 plies of laminates applied to all the square columns and extended for a length larger than the effective plastic hinge length, about 380 mm, computed

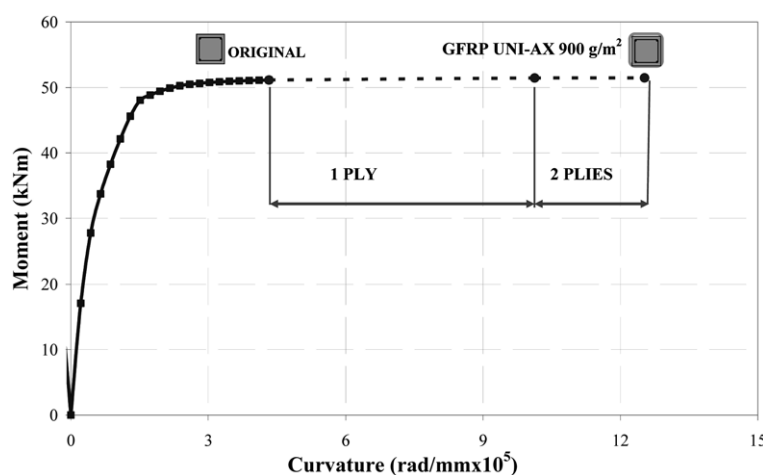


Fig. 4 Moment-curvature relationship of column C3 at first story ( $P = 409$  kN): un-reinforced cross-section (continuous line) and GFRP confined cross-section (dashed line)



following expression given by the Ordinanza 3431 (2005).

Furthermore, in order to validate such design choice, a non linear static pushover on the FRP retrofitted structure was provided at the end of the design process.

As concern the second retrofit goal, in order to avoid that increasing the ductility of the columns cause shear failure (that is brittle and could be detrimental to the global performance of the structure) of exterior joints or of the rectangular column C6, further FRP local interventions were designed.

In particular, with reference to the beam-column joints corresponding to the corner square columns C2, C5, C7 and C8, the shear improvement provided by FRP laminates was assessed according to the approach proposed by Antonopoulos and Triantafillou (2002). Considering that increasing the joint strains, the inclination of principal tensile stresses,  $\theta$ , change considerably, it was decided to upgrade the exterior joints by using quadriaxial laminates; according to the columns retrofit, glass fibers were chosen.

Moreover, by using Antonopoulos and Triantafillou (2002) approach it was computed that two plies of GFRP quadriaxial laminates with density of  $1140 \text{ gr/m}^2$ , thickness of dry fibers of  $0.1096 \text{ mm/ply-direction}$ , modulus of elasticity of  $65.7 \text{ GPa}$ , tensile strength of  $986 \text{ MPa}$  and ultimate strain of  $0.015$  were necessary to strongly increase the original shear strength (for the weakest joint an increase of about  $147\%$  is obtained) of the external joints (see Di Ludovico *et al.* 2006).

Finally, since rectangular column C6 has a sectional aspect ratio equal to 3, shear could have controlled its behaviour rather than flexure. For this reason, a shear FRP retrofit was considered necessary. It was computed (by using CNR-DT 200 (2004) provisions) that totally wrapping of rectangular column C6 for its entire length with two plies of the same quadri-axial GFRP laminates used for the above mentioned joints, is able to increase the sectional shear strength by a factor of about  $50\%$ .

As above mentioned, at the end of the design process, a non-linear static pushover analysis was performed with reference to the FRP confined structure in order to estimate the effectiveness of the proposed retrofit technique on the structural global behaviour. Assuming that the story masses remain constant after the FRP retrofit intervention, the modal displacements values in correspondence of each centre of mass in the X and Y direction along with the corresponding normalized lateral loads are the same of those referred to the 'as-built' structure.

The FRP confinement was taken into account by modifying the inelastic flexural behaviour of the elements in correspondence of the member ends, where the plasticity is assumed concentrated (i.e., lumped plasticity model). The bilinear moment – rotation relationship used for each plastic hinge was, in fact, modified by considering the increase of the ultimate curvature  $\phi_u$  (and the related increase of the ultimate rotation capacity) due to the FRP confinement. In particular, it is noted that yielding curvature,  $\phi_y$ , and moment  $M_y$ , were not modified by the FRP confinement, while the ultimate curvature,  $\phi_u$ , and ultimate moment,  $M_u$ , were determined in correspondence of the attainment of the increased ultimate strains in concrete,  $\varepsilon_{ccu}$  (computed from expression provided by the CNR-DT 200 guidelines (2004)) or in the steel reinforcement, assumed equal to  $40\%$  as in the 'as-built' structure.

Plastic hinge length, yielding and ultimate rotation were computed by using the same expression used in the case of the 'as-built' structure. Both LSDL and LSSD were again investigated for the assessment of the structural capacity at both  $0.20g$  and  $0.30g$  PGA level in the PX - NX and PY - NY direction, respectively. The pushover curves on the FRP retrofitted structure for each direction analyzed are reported in Fig. 2. The theoretical results in terms of maximum base shear,  $F_{max}$ , top

displacement,  $d_{\max}$ , and absolute inter-storey drifts are summarized in the left hand side of Table 3. The seismic demand was computed with reference to the same design spectra analyzed in the ‘as-built’ configuration scaled to 0.20g and 0.30g PGA level, respectively. The results in terms of top displacement required for each investigated limit state and PGA level for each direction are also summarized in Table 3.

Such table shows that the FRP retrofitted structure is able to satisfy the LSSD in each direction with reference to both 0.20g and 0.30g PGA level; in particular it is underlined that the verification is satisfied also in the NX direction where the maximum gap in terms of displacement demand was recorded for the ‘as-built’ structure.

Table 3 Summary of the results in terms of capacity and demand for the FRP and RC jacketing rehabilitated structure

Push Direction	Limit State	FRP Rehabilitated Structure				RC Jacketing Rehabilitated Structure			
		Capacity		Demand		Capacity		Demand	
		$F_{\max}$ [KN]	$d_{\max}$ [m]	0,20g	0,30g	$F_{\max}$ [KN]	$d_{\max}$ [m]	0,20g	0,30g
				$d_{\max}$ [m]	$d_{\max}$ [m]			$d_{\max}$ [m]	$d_{\max}$ [m]
PX	LSDL	233	0.0338	0.0248	0.0372*	370	0.0321	0.0164	0.0253
	LSSD	235	0.1182	0.0626	0.0939	390	0.0721	0.0493	0.0740*
NX	LSDL	235	0.0416	0.0247	0.0371	350	0.0367	0.0215	0.0322
	LSSD	235	0.1076	0.0618	0.0927	369	0.0807	0.0584	0.0876*
PY	LSDL	252	0.0421	0.0240	0.0360	372	0.0385	0.0196	0.0294
	LSSD	253	0.1201	0.0610	0.0917	403	0.0893	0.0552	0.0828
NY	LSDL	293	0.0434	0.0240	0.0361	389	0.0401	0.0212	0.0318
	LSSD	294	0.0908	0.0604	0.0906	418	0.0817	0.0578	0.0867*

(\*Demand displacements not satisfied by the retrofitted structure)

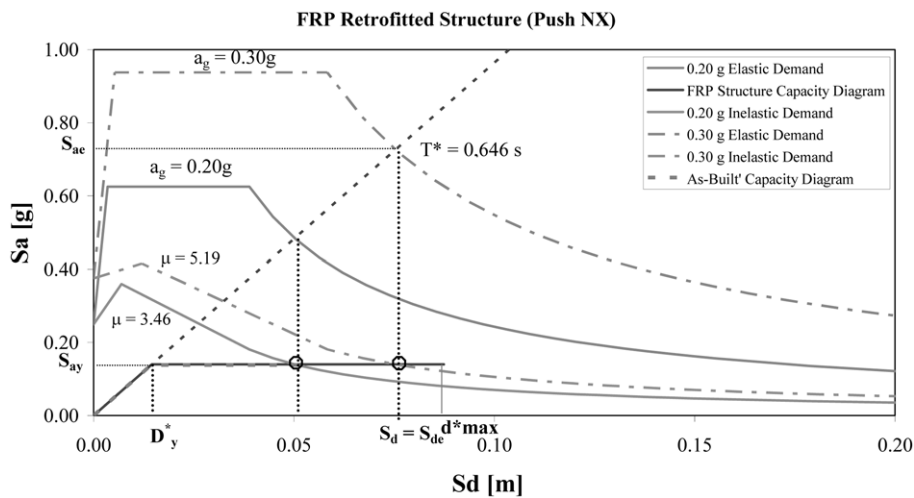


Fig. 5 Elastic and inelastic demand spectra vs. capacity diagram for the FRP retrofitted structure

The capacity, in fact, increases up to a value of 0.1076 m (about 72% larger than that of the ‘as-built structure’, 0.0626 m) while the demand at the target seismic level intensity, 0.30g, is again equal to 0.0927 m (because FRP does not change the elastic period if the idealized bilinear system). The visualization of such result is reported in Fig. 5, where the seismic demand and structural capacity of the FRP retrofitted structure, for the two levels of ground motion analysed, is determined in the NX direction by using the capacity spectrum approach, CSA; at 0.30g PGA level the structural ductility  $\mu_s = d_{\max}^*/D_y^* = 0.0874/0.0145 = 6.02$  exceeds the requested ductility equal to 5.19).

It is noted, however, that although the retrofit intervention provides the structure with the necessary ductility to sustain the 0.30g PGA seismic actions at the LSSD, it is not effective with reference to the damage limit state (i.e., the LSDL verification in the PX direction is again not satisfied also in the retrofitted configuration).

### 3.2 RC Jacketing

The aim of the second rehabilitation strategy was to increase both strength and ductility capacity of the ‘as-built’ structure by the RC jacketing of selected vertical elements. The choice of the columns to be strengthened was aimed at minimizing the structural torsional effects due to the doubly non-symmetric plan configuration of the ‘as-built’ structure. In this way, it is possible to reduce the displacement demand on the external columns. According to previous research in the field, Rutenberg *et al.* (2002), it was found that, in the inelastic range of the response, the torsional effects are mainly governed by strength eccentricity rather than stiffness eccentricity; thus, the design was aimed at decreasing the eccentricity between the centre of mass, CM, and the centre of strength, CP, at each floor of the structure. The centre of strength was considered as the centre of the columns yielding moments. According to such goal, it was decided to increase the original cross-section of columns C4 and C1 from 250 × 250 mm to the jacketed 400 × 400 mm (i.e., the

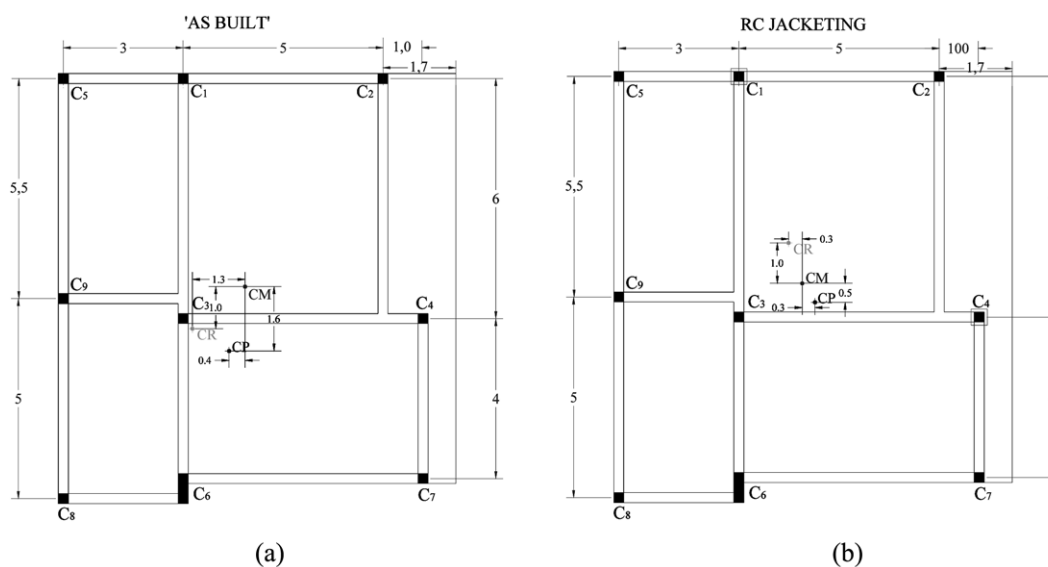


Fig. 6 Eccentricity of stiffness and strength centre: ‘as-built’ structure (a); RC jacketed structure (b) (dimensions in meters)

eccentricity of the CP becomes 0.3 m and 0.5 m instead of 0.4 m and 1.6 m in the X and Y direction, respectively as shown in Fig. 6). Moreover, it is noted that such intervention allows strongly reducing also the eccentricity of the centre of stiffness, CR, in the X direction.

The RC concrete jacketing of column C4 and C1 was designed with shrinkage-compensated concrete design strength equal to  $f'_c = 50$  MPa. The longitudinal reinforcement of the jacketed columns was designed as 3 bars 16 mm diameter for each side of the column and a single leg 8 mm stirrups at 100 mm o.c. at the top and the bottom of the columns (for a length equal to 700 mm starting from the slab) and 150 mm o.c. for the remaining column length; steel bars and stirrups design strength were  $f_y = 430$  MPa.

In order to investigate the performances of the RC jacketed structure, a non linear static pushover was conducted. To model the RC jacketed structure it was necessary to consider that, as a consequence of the columns enlargement, storey masses and centre of masses at each floor change significantly (the storey mass increases from 65.9 tons up to 67.2 tons for the 1<sup>st</sup> and 2<sup>nd</sup> floor and from 63.3 tons up to 63.9 tons for the 3<sup>rd</sup> floor) inducing different initial values of lateral forces. Moreover in the bilinear moment – rotation relationship used for modelling the lumped plasticity at the members ends, both  $\phi_y$  and  $M_y$  as well as  $\phi_u$  and  $M_u$  were modified according to the following assumptions (Ordinanza 3431 (2005) and *fib* Bulletin 24 (2003)): 1) the member was considered as monolithic with full composite action between old and new concrete; 2) concrete strength was taken as that of the old column because the large differences in strength between old and new concrete; 3) axial load was considered acting on the full composite section; 4) the longitudinal reinforcement of the jacket was considered as the reinforcement of the cross-section whereas the reinforcement of the old column was neglected.

Based on such assumptions, and considering that concrete jacketing implies different axial loads values on the columns (due to gravity loads only), yielding and ultimate curvatures (and the corresponding moments) were determined in correspondence of the attainment of the tensile steel yielding strain and of ultimate strains in concrete (conventionally assumed equal to 3.5‰) or steel (equal to 40‰), respectively for each structural member. The moment-curvature relationships for column C4 cross-section in both original and RC jacketed configuration are reported in Fig. 7. Plastic hinge length, yielding and ultimate rotation were again computed by using the expression provided by Ordinanza 3431 (2005). As for the previous analyzed cases, both LSDL and LSSD were investigated for the assessment of the structural capacity at both 0.20g and 0.30g PGA level in the PX - NX and PY - NY direction, respectively. The pushover curves on the RC jacketed structure for each direction analyzed are reported in Fig. 2. The theoretical results in terms of maximum base shear,  $F_{max}$ , top displacement,  $d_{max}$ , and absolute inter-storey drifts are summarized in the right-side hand of Table 3. In the same table, the seismic demand corresponding to the 0.20 g and 0.30 g PGA level in terms of top displacement are also reported.

Such table shows that RC jacketing allows the structure satisfying the LSDL at both 0.20 g and 0.30 g in each direction; it is shown, in fact, that in the PX direction for the 0.30 g PGA level (for which the ‘as-built’ structure was unable to satisfy the seismic demand) even though the top displacement capacity is less than that of the ‘as-built’ structure (0.0321 m vs. 0.0355 m), the structure can sustain the displacement demand that is now strongly decreased from a value of 0.0372 m up to 0.0253 m. Such effect is obviously due to the stiffness increase provided by the RC jacketing that produces an elastic period decrease and thus allows reducing the seismic demand (i.e., the elastic period of the idealized bilinear system is  $T^* = 0.646$ s for the ‘as-built’ structure and  $T^* = 0.606$ s for the jacketed one).

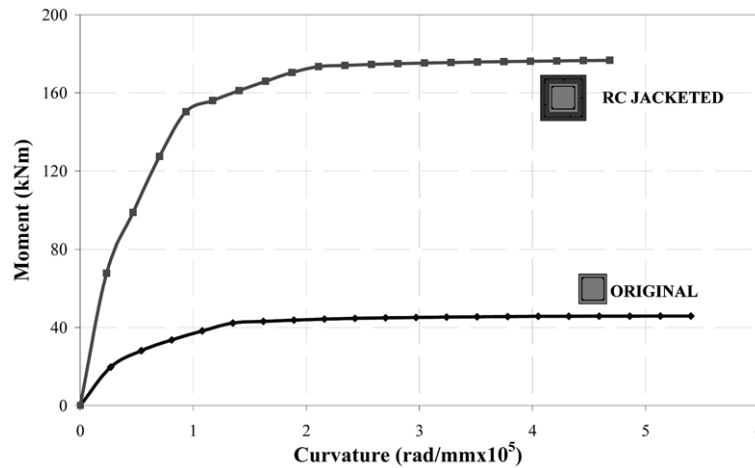


Fig. 7 Moment-curvature relationship of column C4 at first story ( $P = 328$  kN): original cross-section and GFRP confined cross-section

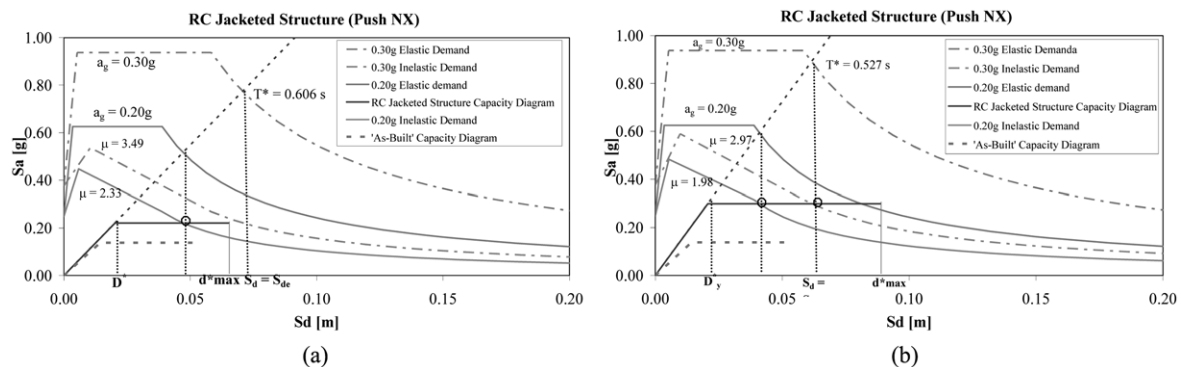


Fig. 8 Elastic and inelastic demand spectra vs. capacity diagram: jacketing of columns C1 and C4 (a), jacketing of external columns (b)

As concerns the LSDS verifications, Table 3 shows that the rehabilitation intervention, although increases significantly both ductility and strength of the 'as-built' structure, it is slightly insufficient to allow the structure, except for the PY direction, withstanding the demand due to the seismic action at 0.30g PGA level. Such result can be observed for the NX direction in Fig. 8(a) in which the seismic demand and the structural capacity are plotted and compared by using the CSA approach; the requested ductility at 0.30g PGA level is equal to 3.49 against the structural ductility  $\mu_s = d_{\max}^*/D_y^* = 0.0651/0.0202 = 3.21$  (ductility gap equal to 9%).

As a consequence, it was decided to investigate on the effectiveness of a more invasive scheme of RC jacketing with the aim of a further mitigation of the strength eccentricities and increase of the global deformation capacity of the structure. Thus, it was analyzed the effect of the jacketing of the seven square perimeter columns to 400 mm (Kosmopoulos *et al.* 2004). By such intervention, in fact, the eccentricity of the CP in the Y direction could be minimised up to a value of 0.25 m (that is half of that of the previous analysed rehabilitation scheme). A non linear static pushover was again performed and it was found that such retrofit resulted much more effective in preventing

structural damage because it could determine a substantial increase of the structural global deformation capacity. In particular, it appeared quite excessive as provides the structure in the NX direction with an available ductility equal to  $\mu_s = d_{\max}^*/D_y^* = 0.0887/0.0207 = 4.28$  that is about 44% larger than the requested one at 0.30g,  $\mu = 2.97$  (see Fig. 8(b)). Taking into account also that the first RC jacketing option is lighter as far as the impact of the retrofitting and it is much easier and faster to implement both in the field and in the laboratory, it was decided to follow the first RC jacketing option outlined (enlargement of square columns C4 and C1 to 400 mm).

#### 4. Experimental behaviour of the rehabilitated structures

Once testing of the ‘as-built’ structure and the design of the two rehabilitation strategies was completed, experimental tests were conducted at both 0.20g and 0.30g on the two rehabilitated configurations. Such second round of tests started on the FRP retrofitted structure; then another phase was performed on the RC jacketed structure. The main experimental outcomes are illustrated in the following sections. A comparison between the experimental results and the theoretical prediction is also performed. However, it is noted that the performed nonlinear static pushover analysis implemented on the structure lumped plasticity model has not been developed as a direct comparison tool with the experimental results but in the way of an effective rehabilitation design methodology supported by a qualitative experimental feed-back.

##### 4.1 FRP Retrofitted structure

After the test on the ‘as-built’ structure, prior to laminates installation, unsound concrete was removed in all zones of the elements where crushing was detected; then the original cross-sections were restored using a non-shrinking mortar. In addition, all cracks caused by the first round of test were epoxy-injected. Then, according to the design of the retrofit above illustrated, the eight square columns were all confined at the top and bottom (for 800 mm from the beam-column interface) using 2 plies of GFRP uniaxial laminates having each a density of 900 gr/m<sup>2</sup> (see Fig. 9(a)). Beam-column joints corresponding to the corner square columns (C2, C5, C7 and C8) were strengthened using 2 plies of quadriaxial GFRP laminates having each a balanced density of 1140 gr/m<sup>2</sup>. This joint reinforcement was extended to the beams by 200 mm on each side in order to U-wrap it and to ensure a proper bond (see Figs. 9(b-c)). The external reinforcement on the joints was not connected to the columns; the continuity of external reinforcement, in fact, can vary the strength hierarchy of the connection and reduce the contribution of fixed end rotation to the rotation capacity of column (therefore the plastic hinge length of rehabilitated columns was assumed comparable with those of the ‘as-built’ structure). Finally column C6 was wrapped for its entire height by using the same quadriaxial laminates provided in the joints (see Fig. 9(d)).

Once FRP-retrofitted, the structure was first tested under the same input ground motion of the ‘as-built’ structure, with a PGA level of 0.20g, then with a PGA level of 0.30g.

The experimental outcomes highlighted a very similar behaviour between the ‘as built’ and retrofitted structure with reference to the same seismic level intensity (0.20g) confirming that, as masses and strength were not significantly changed, the retrofit intervention did not modify the structural response. However, increasing the seismic level intensity at value of 0.30g, it was observed that the retrofitting intervention provided the structure with a very significant supply of

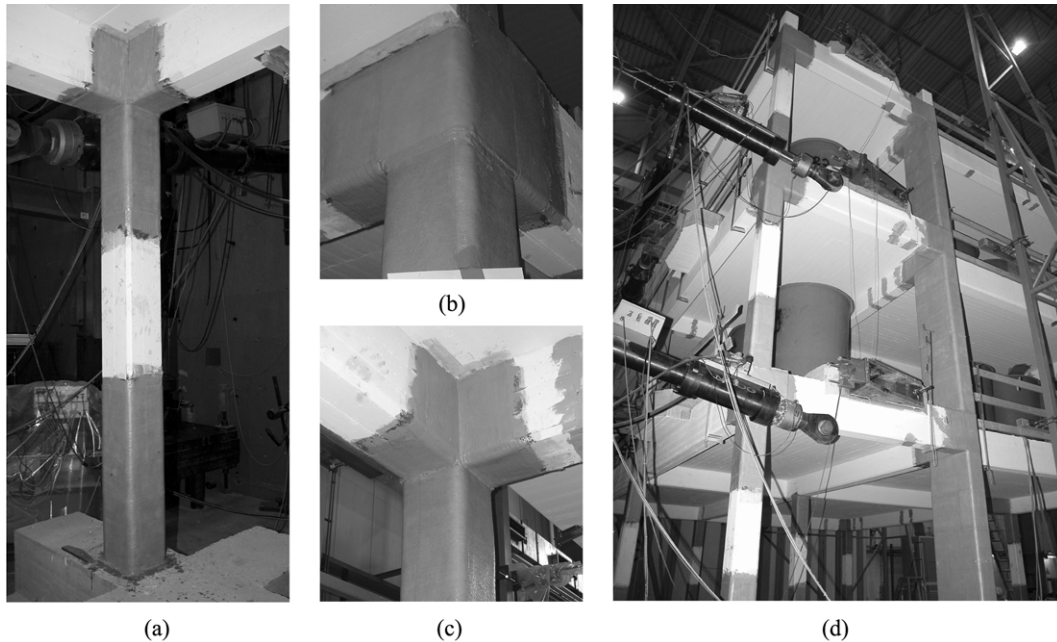


Fig. 9 FRP column confinement (a) and shear strengthening of exterior joints ((b) and (c)) and wall-type column C6 (d)

extra ductility with respect to the ‘as built’ configuration, which was almost totally lacking the appropriate capacity to resist even the 0.20g PGA level of excitation. The retrofitted structure, in fact, was able to withstand the higher (0.30g PGA) level of excitation without exhibiting relevant damage (Balsamo *et al.* 2005).

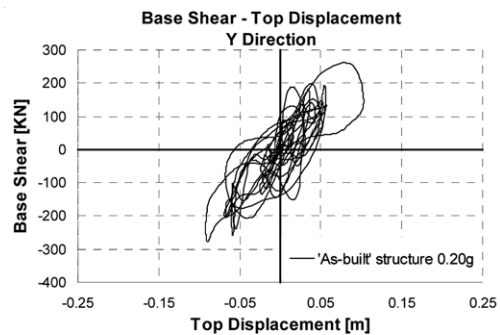
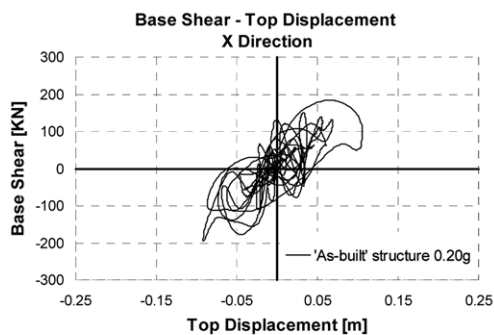
Although the maximum base shear recorded was almost the same as that of the previous test, the displacement capacity of the structure was significantly enhanced, especially in the X direction, where the maximum top displacement recorded was equal to 0.2053 m (see Table 4), roughly two times that reached during the test on the ‘as-built’ structure.

Such result is clearly pointed out in Fig. 10 where the base shear-top displacement curves (for the X and Y direction) are presented for the FRP retrofitted structure at 0.30g PGA level and compared with those recorded in the test performed on the ‘as-built’ structure (0.20g). Moreover, considering that by totaling up the areas under hysteretic cycles of base shear-top displacement relationships it is possible to compute the energy dissipation, such figure indicates that the absorbed energy by the FRP retrofitted structure was equal to 83.36 kJ and 104.38 kJ for the X and Y direction respectively with an increment of the 89% and 61% compared to the results obtained during the test on the ‘as-built’ structure (44.0 kJ and 65.0 kJ in longitudinal and transverse direction).

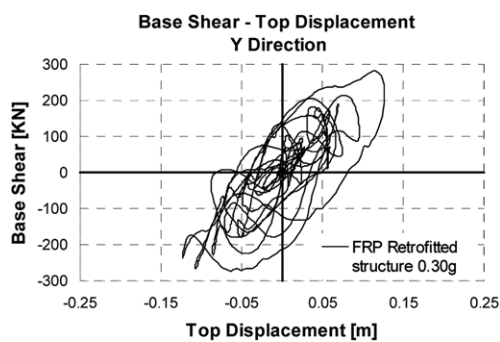
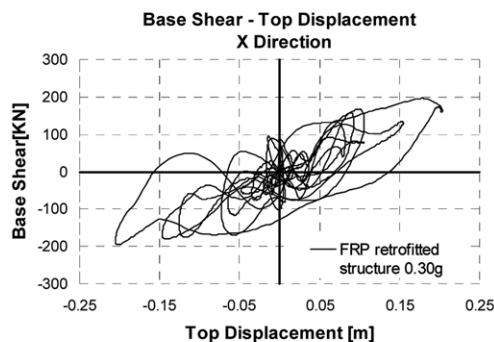
Such results confirm that the FRP retrofit is able to strongly increase the global ductility of the structure slightly affecting its strength. Further experimental evidences are attained if the results in terms of absolutely inter-storey drifts for the structure in the two configurations are analyzed; a significant increase of absolute inter-storey drift was recorded at each floor comparing the values recorded at the 0.3g PGA in the FRP retrofitted configuration with those at 0.20g PGA in the ‘as-built’ configuration; in particular an increase of about 85% was recorded at the second storey in the weak direction X (0.1060 m vs. 0.0570 m).

Table 4 Experimental outcomes in the retrofitted configurations (0.30g PGA level)

	Test	Max Base Shear [kN]	Max Base Shear [m]	Level	Max I-S Displ. [m]
X Direction	FRP Retrofit 0.3g	PX: 196	PX: 0.2036	1	0.0594
				2	0.1060
		NX: 197	NX: 0.2053	3	0.0635
	RC Jacketing 0.3g	PX: 268	PX: 0.0896	1	0.0586
				2	0.0673
		NX: 278	NX: 0.1616	3	0.0362
Y Direction	FRP Retrofit 0.3g	PY: 281	PY: 0.1266	1	0.0423
				2	0.0559
		NY: 273	NY: 0.1233	3	0.0507
	RC Jacketing 0.3g	PY: 355	PY: 0.1117	1	0.0427
				2	0.0549
		NY: 375	NY: 0.1349	3	0.052



(a) 'As-built' structure X and Y Direction



(b) FRP retrofitted structure X and Y Direction

Fig. 10 Experimental Base-Shear Top-Displacement curves for the 'as-built' structure at PGA level 0.20g (a); and for the FRP retrofitted at PGA level 0.30g (b)



The experimental behaviour of the rehabilitated structure was very close to that expected according to the rehabilitation design: 1) columns showed a very ductile behaviour; 2) no brittle mechanisms occurred (i.e., shear failure or significant damage of joints).

#### 4.2 RC Jacketed structure

After the test on the FRP retrofitted structure, prior to RC concrete jacketing, the FRP laminates installed in the previous round of tests were removed; then RC jacketing of columns C4 and C1 was provided by increasing their cross-section from  $250 \times 250$  mm up to  $400 \times 400$  mm. In order to ensure the effectiveness of the retrofit, the longitudinal reinforcement (8 bars 16 mm diameter) was passed through holes drilled in the slab in the interior corners (see Fig. 11(a)) and, for the bars in correspondence of the beams, anchored within the beams starting to the upper and bottom side of the beams with an overlapping length equal to 100 mm. After that, added stirrups with the designed spacing were placed along the columns and in correspondence of the joints where L-shaped and C-shaped stirrups for column C4 and C1, respectively, were installed (see Figs. 11(b) and (c)). Once the jacketing of the two columns was completed (Fig. 11(d)), the structure was again tested under the PGA level of 0.20g, and 0.30g. The main experimental outcomes in terms of maximum base shear and top displacement along with the maximum inter-storey drifts achieved during the test on the RC retrofitted structure at 0.30g PGA level are summarized in Table 4.

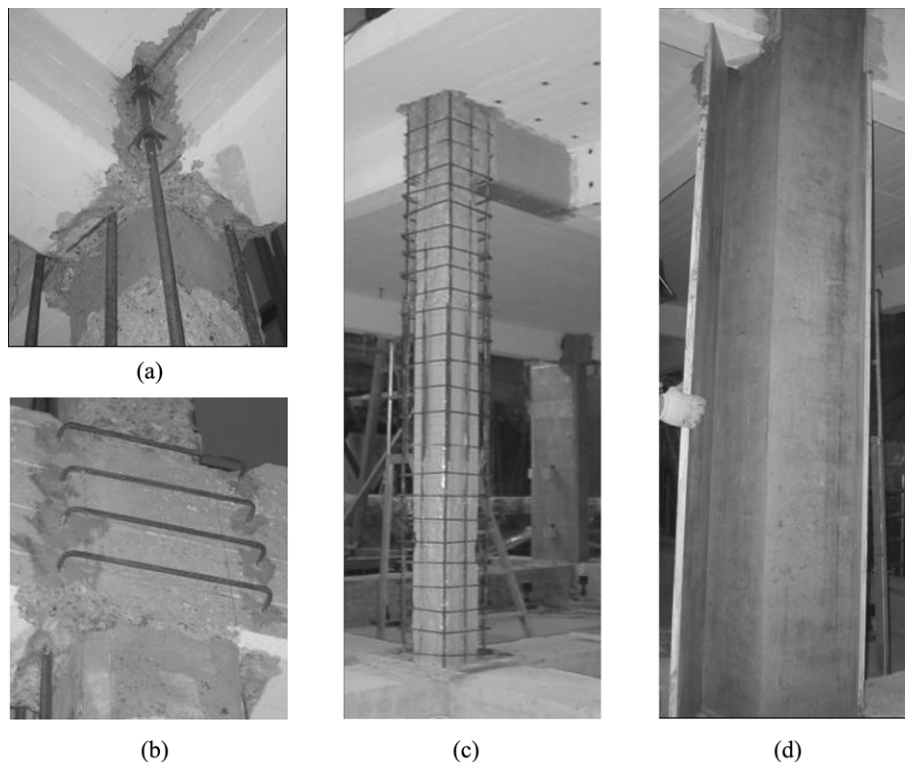


Fig. 11 RC jacketing: added longitudinal reinforcement (a), added stirrups on joints (b); added reinforcement (c); and column after the jacketing (d)

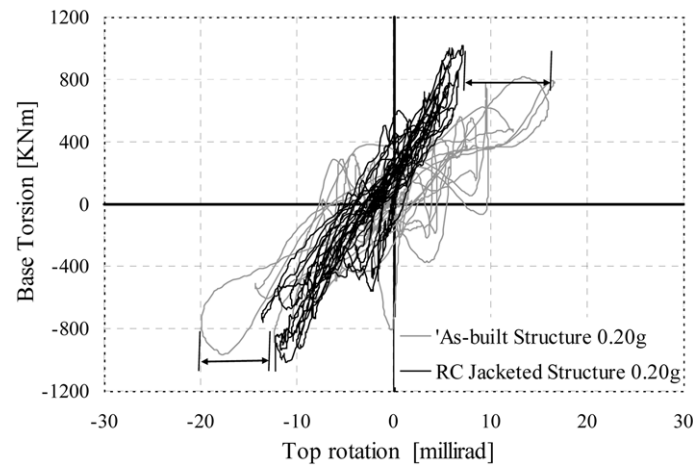


Fig. 12 Experimental Base torsion vs. top rotation: 'as-built' and RC jacketed structure at 0.20 PGA level

Both tests at 0.20g and 0.30g showed that the rotational component of the response was strongly reduced as expected according to the rehabilitation design. Such effect is clearly shown in Fig. 12 in which the base-torsion vs. top rotation curve is plotted for both 'as-built' and RC jacketed structure at PGA level equal to 0.20g.

However, it was observed, by the experimental activity, that such effect was not enough to allow the structure to sustain the high intensity of 0.30g PGA; after the 0.20g test, in fact, significant damages were already detected especially in correspondence of the central column C3, where the axial load was maximum and thus the rotational capacity was limited. Such column showed, at the top of the first storey, a heavy concrete spalling with initiation of buckling of the longitudinal steel rebars (see Mola *et al.* 2005). Increasing the seismic action up to a 0.30g PGA level, such damage became more and more evident until even core concrete crushed; the complete collapse of the element was achieved in correspondence of 12.93 s of the accelerogram (the accelerogram original length was 15 s). Immediately after the collapse of column C3, loads migrated to the nearest column C9 that showed a progressive increase of concrete spalling and buckling of longitudinal steel bars until its collapse. At this stage the test was interrupted for safety reasons. The experimental results confirmed the theoretical predictions indicating that the retrofit intervention, although increased both ductility and strength of the 'as-built' structure, was not completely able to provide the structure with the requested displacement.

In particular, the experimental results have pointed out a damage level on the rehabilitated structure larger than that predicted by the theoretical analyses with the development of a soft storey mechanism; such divergence can be explained considering that the full scale structure was already tested several times before RC jacketing.

## 5. Comparison between FRP laminates and RC jacketing

The experimental activity validated the theoretical predictions and confirmed the effectiveness of the two rehabilitation methods investigated. In particular, the experimental campaign results allow underlying that FRP wrapping of the columns ends provides the structure with a very significant

extra ductility if collapses by brittle failure are prevented. Such result is clearly pointed out in Fig. 13 where the pushover curves referred to the NX direction are reported for the structure in each configuration. The figure shows that the capacity curves of the 'as-built' and FRP rehabilitated structure are fitted together with the only difference of the increased plastic branch in the case of the FRP rehabilitation. The FRP column wrapping, in fact, allows strongly increasing the global ductility without affecting the global stiffness and strength of the structure. Thus, although the global displacement capacity of the structure is significantly enhanced, the seismic demand, depending by the elastic period of the idealized bilinear system, remains substantially constant.

Moreover, such rehabilitation strategy appears very attractive for use in structural application as FRP laminates are very easy to install and effective also in the cases in which time or space restrictions exist. On the other hand, it is recognized that stiffness irregularities cannot be solved by applying FRP laminates. In such field, the columns RC jacketing intervention appears the most appropriate; such method allows minimizing the eccentricities between the centre of mass and stiffness and/or strength and thus can be used to mitigate the torsional effects due to building plan irregularities. Moreover also in the case of service condition problems the RC jacketing is more effective than FRP laminates as it induces a structural stiffness increase that reduces the elastic period of the structure and consequently the seismic demand request. Such effect is clearly pointed out in Fig. 13 where it is shown that the global stiffness of the FRP rehabilitated structure is almost the same of the 'as-built' structure while it is significantly increased in the case of RC jacketed structure.

The RC jacketing intervention is also able to increase both the global strength and ductility of the structure (see Fig. 13) if the added longitudinal reinforcement, placed in the jacket, passes through the beam-column joint ensuring in this way the reinforcement continuity.

As a drawback, such technique may results much more invasive and difficult from a constructability standpoint with a lengthy disruption of the function of the building and its occupants, especially in the case in which a foundation strengthening is needed. During the design, in fact, attention must be paid to the foundation systems as the increased seismic strength capacity

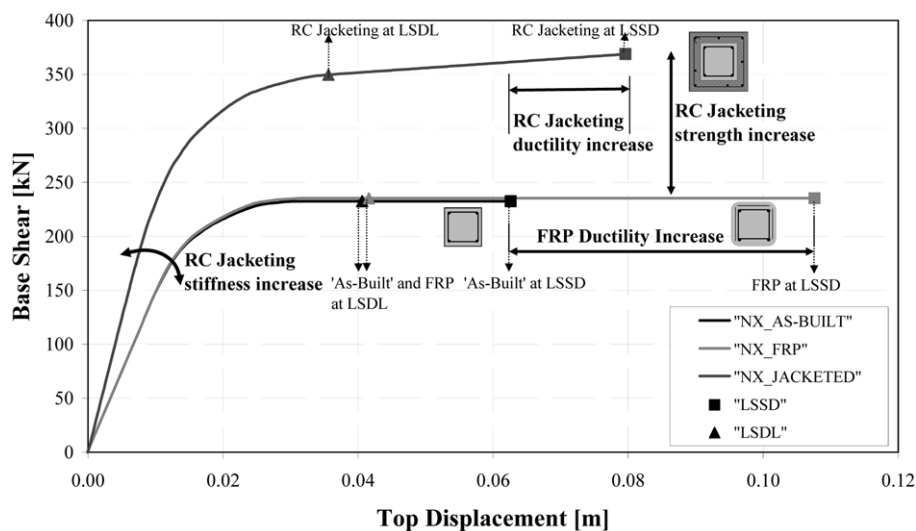


Fig. 13 Pushover curves in the NX direction comparison

leads to an overturning moments increase. When the intervention requires significant upgrade of the foundations its costs could become not affordable or its execution could be not doable.

## **6. Conclusions**

The paper deals with full-scale tests of an under-designed RC structure retrofitted with two different techniques: FRP wrapping of columns and joints and RC jacketing of selected vertical elements. The rehabilitation strategies and criteria followed to improve the seismic performance of the structure were presented and discussed. Theoretical pushover analyses were conducted on both the retrofitted configurations in order to predict the seismic structural behaviour. By the experimental activity conducted on the structure in the three configurations it is possible to point out the following main conclusions:

- FRP laminates intervention (by columns ends wrapping and preventing brittle mechanisms) is a ductility based rehabilitation system: it provided a ductility increase equal to about 123% without varying the structural hierarchy of strength and the elastic period of the structure; it does not affect the torsional behaviour of the structure.
- RC jacketing intervention is a strength-ductility based rehabilitation system: it provided a ductility increase equal to about 76% and a strength increase equal to about 43% with an elastic period decrease of about 25%; it allowed reducing the torsional behaviour of the structure by a factor of about 56%.
- FRP laminates intervention allowed the structure withstanding a level of excitation, in two directions, 1.5 times higher than that applied to the 'as built' structure without exhibiting significant damage or structural deterioration.
- the RC jacketing rehabilitation scheme was strongly effective in mitigating the torsional effects and increasing the seismic performance of the 'as-built' structure especially with regard to the damage limit state; on the other hand such intervention resulted insufficient to fully satisfy the seismic demand in terms of significant damage limitation limit state.

Seismic code provisions, theoretical assumption in the modelling of the structure and for the design of the rehabilitation were validated by the experimental activity conducted on the full-scale structure, such validation provides the opportunity of selecting the most appropriate technique for the seismic retrofit of existing RC frames using either composite materials or traditional techniques.

## **Acknowledgements**

The SPEAR project was co-ordinated by Dr. Paolo Negro, from the Joint Research Centre with the administrative co-ordination of Prof. Michael Fardis, from the University of Patras. Professor Fardis also provided the original design of the structure and the RC jacketing retrofit. The results of the SPEAR project are a joint effort of the whole SPEAR consortium. The pseudodynamic tests were made possible thanks to the expertise and dedication of the whole ELSA staff. The retrofit of the structure was supported by MAPEI S.p.a., Milano, Italy.

## References

- Antonopoulos, C.P. and Triantafyllou, T.C. (2002), "Analysis of FRP-strengthened RC beam-column joints", *J. Comp. Const.*, ASCE, **6**(1), 41-51.
- Balsamo, A., Manfredi, G., Mola, E., Negro, P. and Prota, A. (2005), "Seismic rehabilitation of a full-scale structure using GFRP laminates", *ACI Struct. J. Special Publication*, **230**, 1325-1344, October 1.
- CNR-DT 200 (2004), Guide for the Design and Construction of Externally Bonded FRP Systems for Strengthening Existing Structures.
- CSI SAP 2000 V-7.1 (2002), "Integrated finite element analysis and design of structures basic analysis reference manual", Manual Computer and Structures Inc., Berkley, CA, U.S.A.
- Di Ludovico, M., Prota, A., Manfredi, G. and Cosenza, E. (2006), "Seismic strengthening of an under-designed RC structure with FRP", *Earthq. Eng. Struct. Dyn.*, (in press).
- European Standard, EN 1998-3, Eurocode 8 (2003), "Design of structures for earthquake resistance", *Part 3: Strengthening and Repair of buildings*, Doc CEN/TC250/SC8/N343, Draft No. 3, January.
- Fajfar, P. (2000), "A nonlinear analysis method for performance based seismic design", *Earthq. Spectra*, **16**(3), 573-592.
- Fardis, M.N. (1994), "Analysis and design of reinforced concrete buildings according to Eurocode 2 and 8", Configuration 3, 5 and 6, Reports on Prenormative Research in Support of Eurocode 8.
- Fib Bulletin 24, Task Group 7.1 (2003), Seismic Assessment and Retrofit of Reinforced Concrete Buildings. May.
- Jeong, S.H. and Elnashi, A.S. (2005), "Analytical assessment of an irregular RC frame for full-scale 3D pseudo-dynamic testing-Part I: Analytical model verification", *J. Earthq. Eng.*, **9**(1), 95-128.
- Kosmopoulos, A. and Fardis, N. (2004), "Conceptual design and evaluation of alternative drastic retrofitting schemes of the SPEAR 3-storey test structure", Spear Report.
- Mola, E. and Negro, P. (2005), "Full scale PsD testing of the torsionally unbalanced SPEAR structure in the 'as-built' and retrofitted configurations", *Proc. of the SPEAR International Workshop*, Ispra, Italy, 4-5 April.
- Molina, F.J., Buchet, Ph., Magonette, G.E., Hubert, O. and Negro, P. (2004), "Bidirectional pseudodynamic technique for testing a three-storey reinforced concrete building", *Proc. of 13th WCEE*, Paper N. 75, Vancouver, Canada, 1-6 August.
- Molina, F.J., Verzeletti, G., Magonette, G., Buchet, Ph. and Geradin, M. (1999), "Bi-directional pseudodynamic test of a full-size three-storey building", *Earthq. Eng. Struct. Dyn.*, **28**.
- Negro, P., Mola, E., Molina, F.J. and Magonette, G.E. (2004), "Full-scale PsD testing of a torsionally unbalanced three-storey non-seismic RC frame", *Proc. of 13th WCEE*, Paper N. 968, Vancouver, Canada, 1-6 August.
- Ordinance n. 3431 (2005), "General criteria for seismic classification of national territory and technical guidelines for structures in seismic zones", 3rd May. (*Ordinanza n. 3431, 3 maggio 2005, Ulteriori modifiche ed integrazioni all'ordinanza del Presidente del Consiglio dei Ministri n. 3274 del 20 marzo 2003, recante 'Primi elementi in materia di criteri generali per la classificazione sismica del territorio nazionale e di normative tecniche per le costruzioni in zona sismica*).
- Rutenberg, A. (2002), "Behaviour of irregular and complex structures, asymmetric structures", *Proc. of 12th European Conf. on Earthquake Engineering*, Paper n. 832, London.
- Thermou, G.E. and Elnashai, A.S. (2006), "Seismic retrofit schemes for Rc Structures and local-global consequences", *Earthq. Eng. Struct. Dyn.*, **8**.